Rev. Roum. Sci. Techn.– Électrotechn. et Énerg.
Vol. **64**, *4*, pp. 323–330, Bucarest, 2019

EXPERIMENTAL VERIFICATION OF A ROBUST MAXIMUM POWER POINT TRACKING CONTROL FOR VARIABLE SPEED WIND TURBINE WITHOUT MECHANICAL SENSOR

AHMED TAHRI[1], SAID HASSAINE[1], SANDRINE MOREAU[2]

Key words: Permanent magnet synchronous generator, Wind turbine, Sensorless control, Maximum power point tracking (MPPT), Backstepping control, Sliding mode observer.

This paper presents a robust sensorless control scheme of permanent magnet synchronous generators (PMSG) wind turbine with two full-scale controllable three phase converter connected to the grid. The main aim is to drive wind turbine at an optimal rotor speed in order to perform maximum power point tracking (MPPT) control of the wind generation system. The proposed strategy combines a nonlinear backstepping control of the PMSG which is based on both feedback laws and Lyapunov theory and a non-linear sliding mode observer (SMO) to estimate the PMSG rotor position in order to perform a sensorless control. The PMSG wind turbine is integrated with the grid through a three phase inverter which is controlled through classical proportional integral (PI) to control the active and reactive power. The proposed method was successfully tested with both simulation and experimental setup using MATLAB and a dSPACE 1104 platform. The obtained simulation and experimental results show clearly the accuracy and the effectiveness of the proposed method.

1. INTRODUCTION

The petroleum crisis and the increasing demand of energy, coupled with the possibility of a reduced supply of conventional fuels, have motivated progress in renewable energy research and applications. Among renewable energy sources, wind energy is currently considered to be the most useful natural energy source because it is abundant and clean. Despite these advantages, the efficiency of wind energy conversion is currently low, and the initial cost for its implementation is still considered high. Therefore, the wind energy cost reduction is essential for the rapid spread of the wind power generation through more efficient, reliable and cost-effective wind energy conversion systems (WECS)[1]. WECS, based on permanent magnet synchronous generator (PMSG) drive, is a promising technology due to its high efficiency and the elimination of gearboxes and the external excitation system [2].

Various wind generator systems based on modern wind turbine concepts are developed and described in literature [3–5], which are all about reducing the cost to the minimum, power maximization and improvement and protection of the environment. The direct-drive PMSG is the attractive solution/technology thanks to its high efficiency and reliability as well as its high power density and torque-inertia ratio [5]. However, the performances of the PMSG system depends on synchronous generator and its control technique.

The principle of the vector control introduced by Blaschke [6] gave good dynamic performances. Therefore, many researches are currently focusing on improving this control type. The main difficulty of the vector control is the speed measurement. Therefore, the present research work focuses on the elimination of such sensor. Indeed, the use of mechanical sensors such as tachometer generators, incremental encoders and resolvers to measure mechanical speed not only reduce reliability but also increase the maintenance cost of the control. Consequently, vector control without a mechanical sensor has become an increasingly important part in industry and research.

Several techniques have been developed for the PMSM sensorless control technology. They can be classified into two types: the estimation method based on observer [7,8] and the high-frequency injection method using the salient effect of the motor [9,10]. The flux linkage estimation method, an extended Kalman filter and the model reference adaptive method are widely used to estimate the rotor position. However, the estimation accuracy and stability of the last method depends on motor model. In [11,12], an adaptive neuro-fuzzy method is provided to improve the accuracy of the position estimation under varying speed with variable PMSG parameters, whereas adaptive neuro-fuzzy inference system (ANFIS) estimator shows better performance and immunity against parameters variation. However, in practice, the problem with fuzzy controllers is that the calculation time and complexity increase strongly with the number of variables. In [13] an adaptive interconnected structure with online parameter estimation is adopted to improve the accuracy of the position estimation. It is based on the interconnection between several observers, satisfying some required properties. However, the convergence of the observer depends on the gains related to the state estimation and the parameter identification of the system.

Considering the circumstances mentioned above, sliding mode observer (SMO) is widely used thanks to its robustness and simplicity, which compensate the dependence of the observer on the model [14,15]. This paper presents an improvement and experimental verification of the sensorless control strategy for a PMSG based wind turbine. The control is based essentially on the backstepping control [10,11,16] of the wind turbine speed by imposing the wind profile while SMO is introduced to estimate the speed of the wind turbine generator. In

[1] Laboratoire de Génie Energétique et Génie Informatique (L2GEGI), Ibn Khaldoun University of Tiaret, Algeria, tahriahmed89@gmail.com
[2] Laboratoire d'Informatique et d'Automatique pour les Systèmes(LIAS), University of Poitiers, France.

addition, the PMSG wind turbine is integrated to the grid through three phase converter which controls the active and the reactive power.

The paper is organized as follows: the wind turbine model is given together with the description of the emulator configuration in Section 2. The control strategy of the studied system is detailed in section 3. Simulation and experimental results are discussed in Section 4 and 5 respectively. Finally, a conclusion is presented in Section 6.

2. SYSTEM DESCRIPTION

The proposed structure of a wind energy conversion system is composed of a wind turbine, a PMSG, two full-scale back-to-back pulse width modulation (PWM) converters and inductance filter, as it is shown in Fig.1. The system is connected to the power grid. The modelling of each component is presented as following

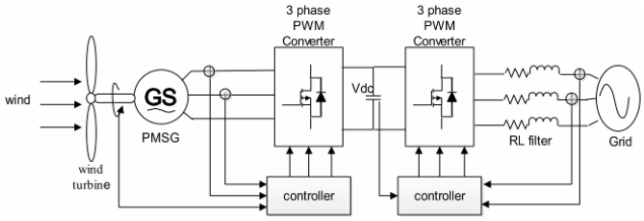

Fig. 1 – The configuration of the wind energy conversion system.

2.1.WIND TURBINE MODEL:

The mechanical power extracted from the wind can be expressed as follows

$$P = \rho\pi R^2 v^3 C_p(\theta,\lambda)/2, \tag{1}$$

where P is the extracted power from the wind, ρ is the air density (kg/m^3), R is the blade radius (m), v is the wind speed (m/s) and C_p is the power coefficient, which is a function of the pitch angle of rotor blades θ (deg) and of the tip speed ratio λ . The term λ is defined as

$$\lambda = \Omega R / v, \tag{2}$$

where Ω is the wind turbine speed. In literature, the power coefficient can be used in the form of look-up tables or in form of a function. The second approach is presented below, where the general function of the power coefficient is defined as a function of the tip-speed ratio λ and the blade pitch angle θ [17]:

$$C_p(\theta,\lambda) = c_1(c_2\frac{1}{\beta} - c_3\theta - c_4\theta^x - c_5)e^{-c_6/\beta}. \tag{3}$$

Since this function depends on the wind turbine rotor type, the coefficients C_i (i =1,2…,6) and x are different for various turbines. the same coefficients as in[13] are used: c_1=0.5, c_2=116, c_3=0.4 , c_4=0, c_5=5,c_6= 21(x is not used because c_4=0). Additionally, the parameter β is also defined in different ways[9] For example, the parameter 1/β is defined as:

$$\frac{1}{\beta} = \frac{1}{(\lambda+0.008)} - \frac{0.035}{1+\theta^3}. \tag{4}$$

2.2.GENERATOR MODEL

The mathematical model of the PSMG is established under the d and q axis synchronous reference frame [13]. It is simplified as:

$$\frac{di_d}{dt} = -\frac{R_s}{L_q}i_d + \frac{\omega_e L_q}{L_d}i_q + \frac{1}{L_d}u_d, \tag{5}$$

$$\frac{di_q}{dt} = -\frac{R_s}{L_q}i_q - \omega_e(\frac{L_d}{L_q}i_d + \frac{1}{L_q}\varphi_f) + \frac{1}{L_q}u_q, \tag{6}$$

where subscripts d and q refer to the physical quantities that have been transformed into the d-q synchronous rotating reference frame, R_s is the stator resistance [Ω], L_d and L_q are the inductances [H] of the generator on the d and q axis. φ_f is the permanent magnetic flux [Wb] and ω_e is the electrical rotating speed [rad/s] of the generator, defined as ω_e=Ω.p , where p is the number of pole pairs and Ω is the rotated speed of the generator.

The electromagnetic torque equation of PMSG is described by this equation:

$$T_e = 3p((L_d - L_q)i_d i_q + i_q\varphi_f)/2. \tag{7}$$

The mechanical equation which connects the generator with the wind turbine is described by:

$$J_{eq}\frac{d\Omega}{dt} = T_e \pm T_l - B_m\Omega, \tag{8}$$

where T_l is the mechanical torque applied by the turbine to the generator. The sign convention of T_l is the following one: when the speed is positive, a positive torque signal indicates the generator mode and a negative signal indicates the motor mode. j_{eq} is the equivalent moment of inertia and B_m is the viscous turn coefficient.

3.CONTROL STRATEGY

It exists two methods to control the PMSG while the wind speed is variable. The first named maximum power point tracking (MPPT), it principle is to make the PMSG running at the speed corresponding to the maximum power point when wind speed is lower than the rated wind speed. While the second method makes the PMSG running around the rated power point by the torque angle controller when the wind speed is higher than the rated wind speed. The torque angle controller is similar to speed controller of generator, which is influenced by the power coefficient C_p [9].

The control strategy of the wind energy converter system is divided in two parts, the first focuses on the control of PMSG by nonlinear backstepping controller relying on the MPPT, and the second part focuses on the control of the active and reactive power injected to the grid, and also on the stabilization of the terminal voltage measured of the capacitor located between the converters; additionally, a sliding mode observer for position is used to eliminate the position sensor.

3.1. CONTROL OF THE PERMANENT MAGNET SYNCHRONOUS GENERATOR SIDE CONVERTER

The control of PMSG is achieved by the nonlinear backstepping controller that is composed of two loops, the inner loop that control the stator current and the outer loop which control the PMSG speed, where the optimum speed reference Ω* is given by the MPPT bloc as shown in Fig. 2.

3.1.1. MPPT PRINCIPLE

The MPPT principle is to extract the maximum of power from the wind power, this can be only realized if the turbine

operates at maximum C_p (*i.e.*, at C_{popt}) [18].Therefore, it is necessary to keep the tip-speed ratio λ at an optimum value λ_{opt} . From (2) to maintain this value it is essential to adjust the rotor speed to an optimum value (Ω_{opt}) in order to follow the change value when the wind varies.

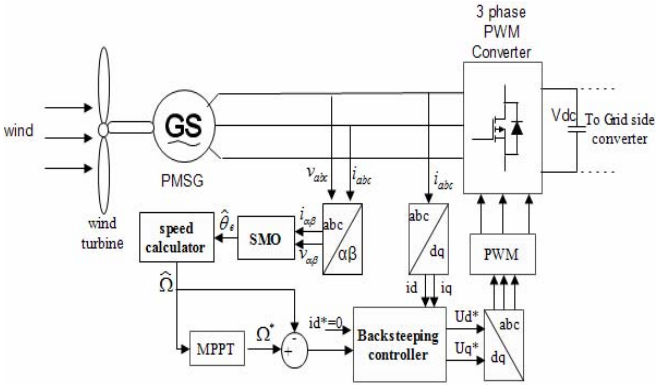

Fig. 2 – Overall diagram of proposed control system of PMSG.

From equations (1) and (2) The optimum power of a wind turbine is written as:

$$p_{\omega_{opt}} = \frac{1}{2}\rho\pi R^2 C_{p_{opt}} \left(\frac{\Omega_{opt}}{\lambda_{opt}}\right)^3, \tag{9}$$

where $\Omega_{opt} = \lambda_{opt} v / R$ and. $\Omega^* = \Omega_{opt} G_r$,

where Ω^* is the PMSG speed reference and G_r is the gear ration of the wind turbine.

3.1.2. BACKSTEPPING CONTROL OF THE PMSG

The backstepping technique is a systematic and recursive method for synthesizing nonlinear control laws. It uses the Lyapunov stability principle which can be applied to a large number of non-linear systems.

The objective of the nonlinear backstepping controller is to track the PMSM speed with the appropriate choice of regulated variables. From [19] the control inputs can be chosen as:

$$u_d = K_1 L_d \varepsilon_d + L_d \frac{\mathrm{d}i_d^*}{\mathrm{d}t} + R_s i_d - \omega_e L_q i_q, \tag{10}$$

$$u_q = K_2 L_q \varepsilon_q + L_q \frac{\mathrm{d}i_q^*}{\mathrm{d}t} + R_s i_q + \omega_e (L_d i_d + \varphi_f), \tag{11}$$

where $\varepsilon_d = e_d + K_d \int_0^t e_d \mathrm{d}t$, $\varepsilon_q = e_q + k_q \int_0^t e_q \mathrm{d}t$

$$e_d = i_d^* - i_d \,, \qquad e_d = i_d^* - i_d \,,$$

where K_1, K_2 are parameters introduced by the backstepping method. They must always be positive and greater than K_d, K_q respectively, to attain the stability criteria of the Lyapunov function. Thus, the virtual control is asymptotically stable. Besides, these parameters can influence the control dynamics and we must select them to ensure that the current dynamics converge faster than the speed ones.

After obtaining the u_d and u_q control signals, they are turned into the three phases voltage reference frame by means of the inverse Park transformation and are given as a reference to the space vector modulation (SVM) block in order to generate the inverter pulse signals.

3.1.3. SLIDING MODE OBSERVER

Unlike conventional design observers, the sliding mode observer for estimating rotor position angle uses only the electrical equations of the PMSM in the fixed coordinate (α,β) due to the fact that angular speed and position information are ready to be extracted in this reference frame [20]. The PMSM model in stationary (αβ) reference frame is

$$\frac{\mathrm{d}i_\alpha}{\mathrm{d}t} = -\frac{R_s}{L_s} i_\alpha - \frac{1}{L_s} e_\alpha + \frac{u_\alpha}{L_s}, \tag{12}$$

$$\frac{\mathrm{d}i_\beta}{\mathrm{d}t} = -\frac{R_s}{L_s} i_\beta - \frac{1}{L_s} e_\beta + \frac{u_\beta}{L_s}, \tag{13}$$

$$e_\alpha = -\varphi_f \omega_e \sin(\theta_e), \tag{14}$$

$$e_\beta = \varphi_f \omega_e \cos(\theta_e). \tag{15}$$

The magnitude (i_α, i_β et u_α, u_β) in the fixed coordinate (αβ) are obtained by the Concordia transformation of the three phase electrical quantities measured (i_a, i_b, i_c and u_a, u_b, u_c) of PMSG as shown in Fig. 2. θ_e is the electrical rotor position of the PMSG and L_s is its stator inductance where L_s=L_α =L_β (because the studied PMSG has nearly a smooth pole).

Equations (12) (13) can be expressed in matrix form as follows

$$\dot{\mathbf{i}}_{\alpha\beta} = \mathbf{A}\mathbf{i}_{\alpha\beta} + \mathbf{B}(\mathbf{u}_{\alpha\beta} - \mathbf{e}_{\alpha\beta}), \tag{16}$$

where

$$\mathbf{A} = \begin{bmatrix} -\frac{R_s}{L_s} & 0 \\ 0 & -\frac{R_s}{L_s} \end{bmatrix}, \qquad \mathbf{B} = \begin{bmatrix} \frac{1}{L_s} & 0 \\ 0 & \frac{1}{L_s} \end{bmatrix}$$

$$\mathbf{i}_{\alpha\beta} = \begin{bmatrix} i_\alpha \\ i_\beta \end{bmatrix}, \qquad \mathbf{u}_{\alpha\beta} = \begin{bmatrix} u_\alpha \\ u_\beta \end{bmatrix}, \qquad \mathbf{e}_{\alpha\beta} = \begin{bmatrix} e_\alpha \\ e_\beta \end{bmatrix}.$$

The sliding mode observer (SMO) is designed in the following form:

$$\dot{\hat{\mathbf{i}}}_{\alpha\beta} = \mathbf{A}\hat{\mathbf{i}}_{\alpha\beta} + \mathbf{B}(\mathbf{u}_{\alpha\beta} + l\mathbf{Z}_{eq} + \mathbf{Z}), \tag{17}$$

where $\mathbf{Z} = -\mathbf{K}\mathrm{sign}(\hat{\mathbf{i}}_{\alpha\beta} - \mathbf{i}_{\alpha\beta})$

In (17) Z_{eq} represents the equivalent control and Z represents the discontinuous control, l is the feedback gain of the equivalent control, and K generally positive ($K > 0$) is the switching gain of the discontinuous control, where the superscript * denotes a control variable and the hat ˆ indicates the estimated variable.

The equivalent control Z_{eq} can be obtained as

$$\mathbf{Z}_{eq} = \begin{bmatrix} Z_{eq\alpha} \\ Z_{eq\beta} \end{bmatrix} = \begin{bmatrix} -K\,\mathrm{sign}(\hat{i}_\alpha - i_\alpha).\frac{\omega_c}{s+\omega_c} \\ -K\,\mathrm{sign}(\hat{i}_\beta - i_\beta).\frac{\omega_c}{s+\omega_c} \end{bmatrix}, \tag{18}$$

where $\omega_c / s + \omega_c$ is a low-pass filter. It is noticed that its cut off frequency ω_c must be properly designed in with respect to the fundamental frequency currents of PMSG.

The sliding surface is selected as $\mathbf{S} = 0$, where:

$$\mathbf{S} = \hat{\mathbf{i}}_{\alpha\beta} - \mathbf{i}_{\alpha\beta} \,.$$

By subtracting equation (16) and (17) we can obtain the dynamic sliding mode motion equation as expressed in

$$\dot{\mathbf{S}} = \mathbf{A}.\mathbf{S} + \mathbf{B}(\mathbf{e}_{\alpha\beta} + l\mathbf{Z}_{\text{eq}} + \mathbf{Z}) \tag{19}$$

If switching gain K is large enough to ensure the following condition:

$$\dot{\mathbf{S}}^{\mathbf{T}}.\mathbf{S} < 0 \tag{20}$$

Then, sliding mode occurs and we get **S**=0 .This implies:

$$\mathbf{e}_{\alpha\beta} = \begin{bmatrix} e_\alpha \\ e_\beta \end{bmatrix} = -(1+l)\mathbf{Z}_{eq} \tag{21}$$

The feedback gain l must be larger than −1 with any positive switching gain K , *i.e.* $l > -1$,which is the limit of the feedback gain of the equivalent control [21]. In our study, the gain l is chosen –0.9. According to (21), we can deduce that the magnitude of the equivalent control Z_{eq} is ten times greater than that of the back EMF. Thus, the rotor position of PMSG is estimated from the equivalent control (Z_{eq}).

At low speeds, the back EMF is weak and the estimated Z_{eq} is enlarged. As a result, observer stability is ensured even in lower speeds and the quality of the estimated rotor position angle is improved.

In addition, from (14) and (15) the angular position of θ_e rotor can be estimated using the equivalent control Z_{eq} as follows:

$$\hat{\theta}_e = -\tan^{-1}\left(\frac{e_\alpha}{e_\beta}\right) = -\tan^{-1}\left(\frac{Z_{eq\alpha}}{Z_{eq\beta}}\right). \tag{22}$$

However, the function sign has some drawback due to the fact that it result a significant chattering, to solve this problem, the function sign is replaced by the function tanh (hyperbolic tangent).

After that, the rotor speed is calculated from the estimation of the rotor position using a numerical derivation.

3.2. CONTROL OF THE GRID SIDE CONVERTER

The role of the grid side converter control is to adjust the dc line voltage to the desired value, and ensure that the output voltage converter has a similar amplitude and frequency with the grid, but the main role of this control is to control the active and reactive power.

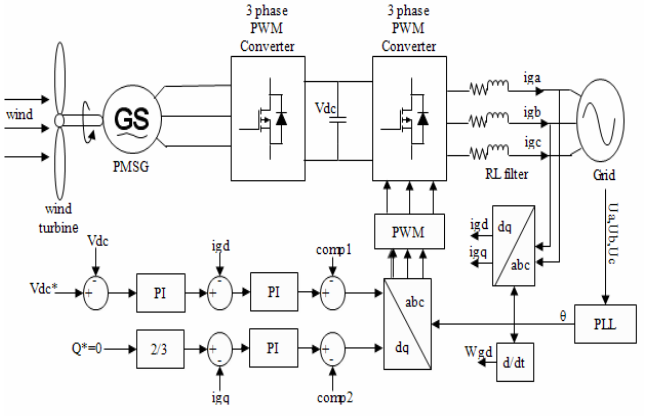

Fig. 3 – Overall diagram of proposed control system of the grid side converter.

3.2.1. DC LINE MODELING AND CONTROL

The dc line is the capacitor located between the convertors; its function is to keep the dc voltage stable, the model of the dc line is expressed as:

$$C\frac{\mathrm{d}V_{dc}}{\mathrm{d}t} = i_s - i_g\,, \tag{23}$$

where V_{dc} is the dc line voltage, i_s is the current of dc line at the generator side and i_g is the current of dc line at the grid side, C is the capacity of dc line capacitor.

Let us suppose that the convertor is ideal *i.e.* does not consume power, the voltage of the capacitor is written as

$$C\frac{\mathrm{d}V_{dc}}{\mathrm{d}t} = \frac{P_s}{V_{dc}} - i_g\,, \tag{24}$$

where P_s is the output power of generator. We can write it as

$$P_s = 3V_s i_s = V_{dc} i_{dc}\,. \tag{25}$$

We rephrase it as

$$P_s = \frac{3}{2}E_{\max}I_{\max} = V_{dc}i_{dc}\,, \tag{26}$$

where V_s is the voltage of generator side and $E_{\max}$ is its amplitude, $I_{\max}$ is the amplitude of the generator current, and i_{dc} is the current through the capacitor.

The control block diagram of the dc line is presented in Fig. 4.

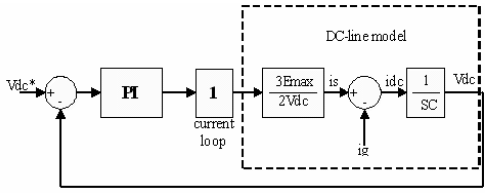

Fig. 4 – Diagram of the loop control of dc line.

In this loop control, the current loop is considered to be faster than the voltage loop. We suppose it as equal to 1.

The proportional integral (PI) controller is designed with the pole placement method.

3.2.2. CONTROL OF ACTIVE AND REACTIVE POWER

The dynamic model of the grid connection when selecting a reference frame rotating synchronously with the grid voltage space vector is

$$u_{gd} = -R_g i_{gd} - L_g\frac{\mathrm{d}i_{gd}}{\mathrm{d}t} + \omega_{gr}L_g i_{gq} + e_{gd}\,, \tag{27}$$

$$u_{gq} = -R_g i_{gq} - L_g\frac{\mathrm{d}i_{gq}}{\mathrm{d}t} - \omega_{gr}L_g i_{gd}\,, \tag{28}$$

where R_g and L_g are the resistance and inductance respectively of the filter, this latter is located between the converter and the grid, u_{gd} and u_{gq} are the inverter voltage components, ω_{gr} is the electrical angular velocity of the grid.

If the reference frame is oriented along the supply voltage, the grid voltage vector is

$$u = u_{gd} + \mathrm{j}0\,. \tag{29}$$

Then active and reactive power goes through the grid side converter, it is written as:

$$P = 3u_{gd}i_{gd}/2\,, \tag{30}$$

$$Q = 3u_{gd}i_{gq}/2. \tag{31}$$

The active and reactive power control is achieved in two loops, by controlling direct and quadrature current components [15] as shown in Fig.3.

In Fig.3, θ_e is the electrical angle of the grid, it is extracted with the phase locked loops (PLL), and

$comp1 = \omega_{gr} L_g i_{gq} + e_{gd}$; $comp2 = \omega_{gr} L_g i_{gd}$ are the compensation terms

The first channel controls the dc voltage which is used to provide to the d axis current reference for active power control. This assures that all the power coming from the PMSG converter is instantly transferred to the grid through the converter.

The second channel controls the reactive power by setting the q axis current reference to the current control loop similar to the previous one. The current controllers will provide a voltage reference for the converter that is compensated by adding rotational electromotive force (EMF) compensation terms. All controllers are PI and are tuned using the pole placement method.

4. SIMULATION RESULTS

The control strategy of the studied wind energy conversion system is investigated using SimPowerSystems of Matlab/simulink.

The system performance and robustness is evaluated for the PMSG parameters shown in Table 1, the main measurements include three-phase stator voltage, and three-phase stator current.

The controller has as input, the speed reference extracted from the MPPT block, the observed speed, the direct and quadrature stator current and also the torque applied by the wind turbine on the PMSG.

Table 1

PMSG parameter

PMSM parameters	**Value**
Rated power	1 kW
Rated line current	7 A
Rated speed	1500 rpm
Mutual inductance L_q	4 mH
Mutual inductance L_d	4.5 mH
Stator resistance R_s	0.57 Ω
Number of pole pairs p	2
Permanent magnet flux φ_f	0.064 Wb
Viscous friction B_m	0.0039 Nm/rad/s
Inertia moment	0.00208 kg.m^2
Turbine parameters	**Value**
Air density ρ	1.22 kg/m^3
Gear ratio	2
Rotor radius R	3 m
Inertia moment J_{eq} (turbine+PMSG)	0.042 kg.m^2

In order to test the robustness of the proposed control system, the used wind speed profile is as shows Fig. 5, it varies between 4 to 9 m/s.

Figure 6 shows the PMSG speed under variable wind speed condition, we can see the good performance of both observer and the backstepping controller, where the response time of the PMSG speed is very short; there is no overshoot and no steady state error. Figures 7 and 8 show the i_d and i_q currents performance where the latter follow perfectly there reference.

The observer performances are shown in Figs. 9 and 10, where the observed PMSG stator current in αβ reference frame is shown in Fig.9, we can see in the zoom of Fig. 9 the good follow of the observed current the measurement one, as we can see in Fig.10 the estimation error is around 5 mA. Figure 11 shows the observed PMSG rotor position and the measurement one, where the observation delay time is very short. The dc line voltage is maintained around their reference (400 V) with no steady state error as shown in Fig.12.

The wind conversion system operates at maximum power as shown in Fig.13 which means that the power coefficient is around the maximum value ($C_{p\max}$=0.41).

Figure14 shows the active power produced by the PMSG.

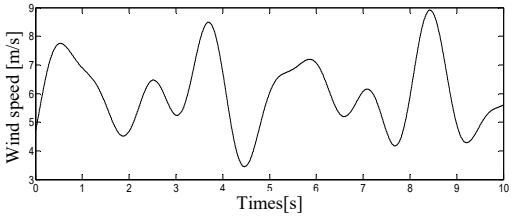

Fig. 5 – Wind speed.

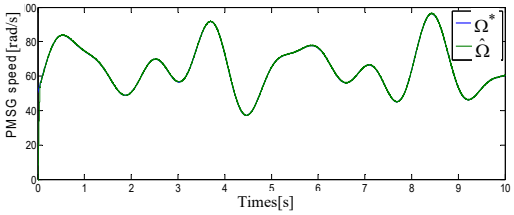

Fig. 6 – Observed PMSG speed.

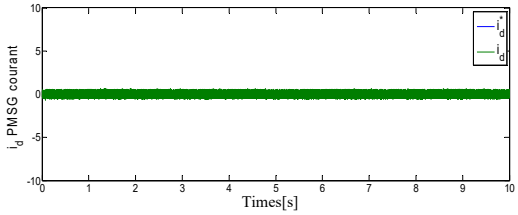

Fig. 7 – PMSG current in d axis (i_d).

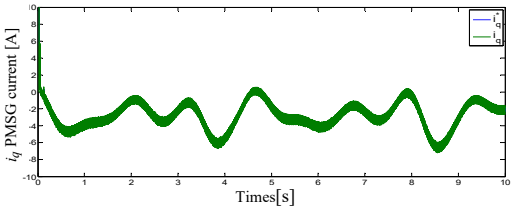

Fig. 8 – PMSG current in q axis (i_q).

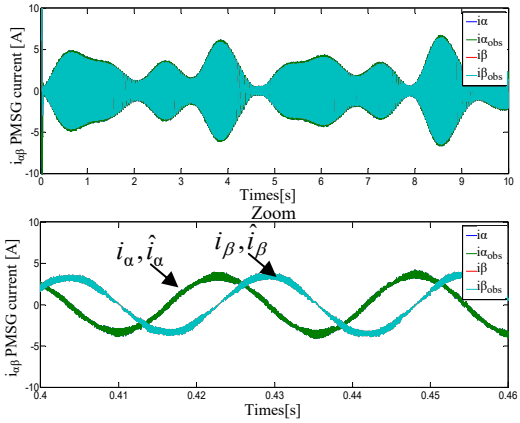

Fig. 9 – Observed and measurement PMSG current in αβ axis.

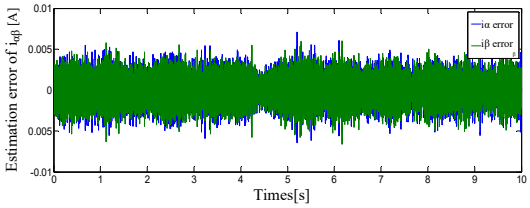

Fig. 10 – Currents estimations errors.

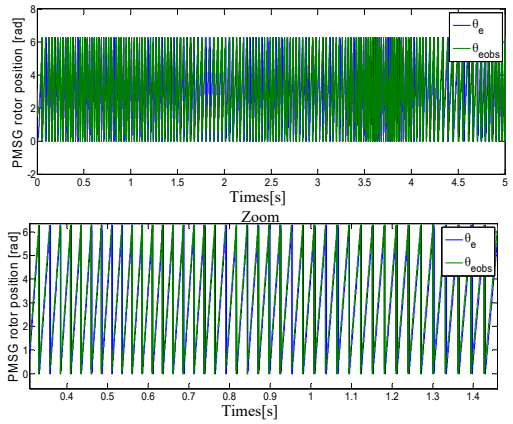

Fig. 11 – Observed PMSG position.

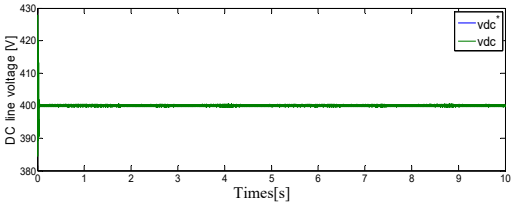

Fig. 12 – Dc line voltage.

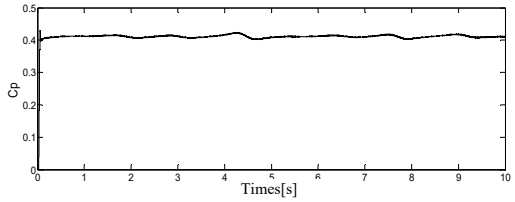

Fig. 13 – Power coefficient (Cp).

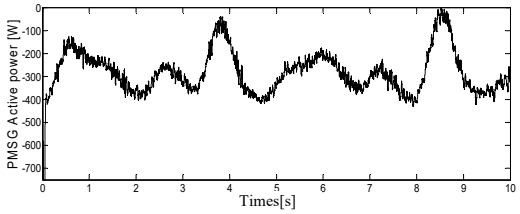

Fig. 14 – Active power produced by the PMSG.

5. EXPERIMENTAL VALIDATION

In order to validate the developed method, a test bench has been set up. The used test bench comprises a PMSG driven by an actuator composed of a PMSM and its power and its control. This set simulates a real wind turbine, by controlling the torque on the shaft and driving the PMSG which delivers the produced energy on a resistive load. A dSPACE DS1104 DSP system is used to carry out the real-time algorithm. The parameters of the PMSG are given in Table 1. The experimental test bench is shown in Fig.15.

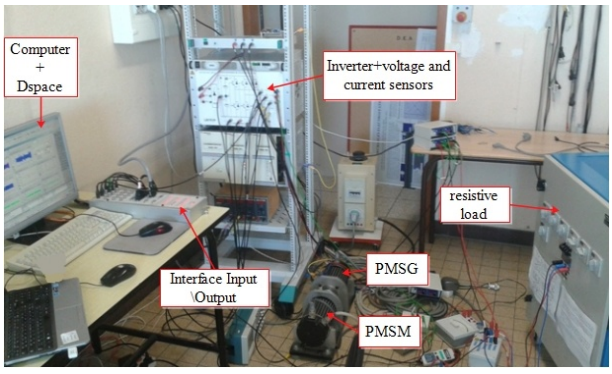

Fig. 15 – Experimental setup.

The speed response of the backstepping controller shows good tracking performances, as shown in Fig.16 when the speed controller operates in variable wind speed and load variation conditions. The load variation is seen in the three phase current of the PMSG and of the emulator as shows the Fig.19 (at 3.5 s and 6.5 s).

Figures 17 and 18 show the response of the currents in the d-axis and q axis. We observe that they follow perfectly their references with good performance. It ensures the good robustness of the backstepping controller. We noticed that there is a chattering phenomenon in the currents, caused by the commutation frequency (at 10 kHz) of the inverter.

Furthermore, we present the observed variables of the generator side which are the speed and the rotor position as shows Fig.16, where we can see that the observers variable follow perfectly the measurement one. Figures 20 and 21 the observed currents in the fixed reference frame (αβ) correspond to the measurement currents with an error approximately null, as shown in Figs. 22 and 23. Therefore, these results prove the robustness of the proposed sliding mode observer.

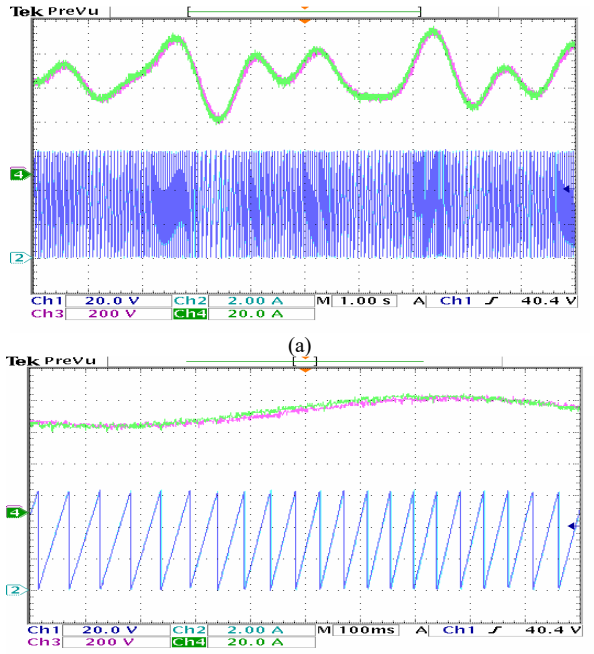

Fig. 16 –(a) SMO performance: Ch1(1rad per div): measured rotor position, Ch2(1 rad per div): Observed position, Ch3(20 rad/s per div): observed speed, Ch4(20 rad/s per div): measured speed. (b) Zoom.

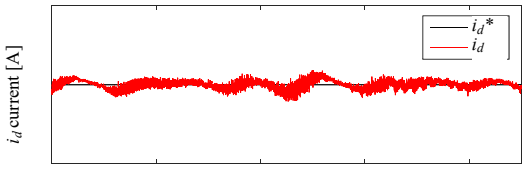

Fig. 17– PMSG current in d axis (i_d).

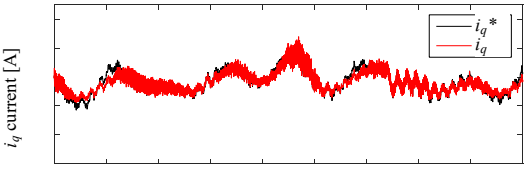

Fig. 18 – PMSG current in q axis (i_q).

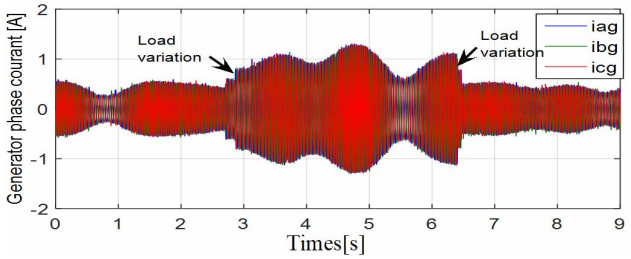

Fig. 19 – The three phase PMSG currents.

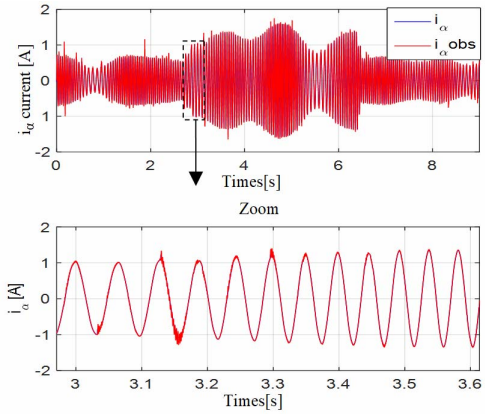

Fig. 20 – PMSG current in α axe (i_{α}) and its observation ($i_{\alpha obs}$).

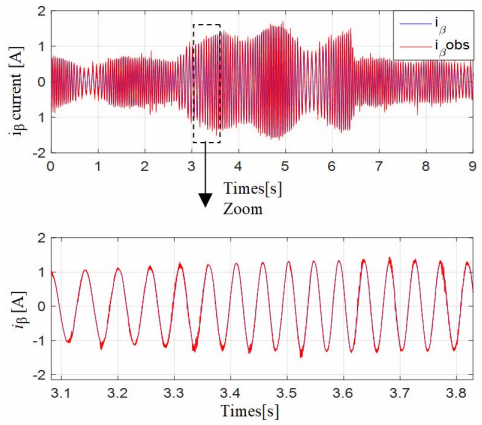

Fig. 21 – PMSG current in β axe (i_{β},)and its observation ($i_{\beta obs}$).

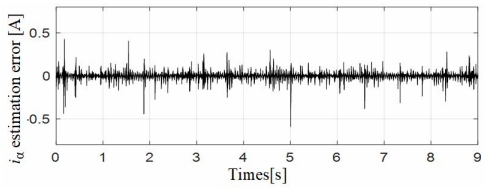

Fig. 22 – Estimation error of i_{α}.

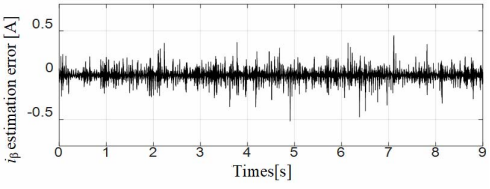

Fig. 23 – Estimation error of i_{β}.

6. CONCLUSION

In this paper, a robust MPPT sensorless control for a wind turbine based PMSG integrated with the grid has been presented. The main objective is to improve the reliability and efficiency of the wind energy conversion system by using a robust MPPT control without mechanical sensor. The proposed method is based on a nonlinear backstepping strategy, combined with a SMO to achieve a sensorless MPPT control. The obtained simulation and experimental results prove the effectiveness of the proposed strategy with a robust stability and transient performances and ability to track the maximum power from the wind power when exciting the system with a variable wind speed. Finally, as a further improvement of the proposed strategy, it will be interesting to apply this approach in a fault operation mode.

ACKNOWLEDGEMENTS

This work has been supported by the Algerian government (PNE scholarship), and the Computer Science and Automatic Control for Systems Laboratory at the University of Poitiers, France.

Received on September 19, 2017

REFERENCES

1. N. M. A. Freire, J. O. Estima, A. J. M. Cardoso, *A new approach for current sensor fault diagnosis in PMSG drives for wind energy conversion systems*, IEEE Energy Conversion Congress and Exposition (ECCE), 2012, pp. 2083–2090.
2. Fatu, Marius, Frede Blaabjerg, Ion Boldea. *Grid to standalone transition motion-sensorless dual-inverter control of PMSG with asymmetrical grid voltage sags and harmonics filtering*. IEEE Transactions on Power Electronics, **29**, *7*, pp. 3463-3472, (2013).
3. A. D. Hansen and L. H. Hansen, *Wind turbine concept market penetration over 10 years (1995–2004)*, Wind Energy, **10**, *1*, pp. 81–97 (2007).
4. H. Li and Z. Chen, *Overview of different wind generator systems and their comparisons*, IET Renew. Power Gener., **2**, *2*, pp. 123–138 (2008).
5. Y. Duan, R. G. Harley, *Present and future trends in wind turbine generator designs*, in IEEE Power Electronics and Machines in Wind Applications, 2009, pp. 1–6.
6. F. Blaschke, *The principle of field orientation as applied to the new transvektor closed-loop control system for rotating field machines*, Siemens review, **34**, *3*, pp.217-220 (1972).
7. H. Li, Z. Chen, H. Polinder, *Optimization of multibrid permanent-magnet wind generator systems*, Energy Convers. IEEE Trans. On, **24**, 1, pp. 82–92 (2009).
8. D. Bang, H. Polinder, G. Shrestha, J. A. Ferreira, *Review of generator systems for direct-drive wind turbines*, in European Wind Energy Conference & Exhibition, Belgium, 2008, pp. 1–11.
9. S. Li, T. A. Haskew,L. Xu, *Conventional and novel control designs for direct driven PMSG wind turbines*, Electr. Power Syst. Res., **80**, *3*, pp. 328–338, (2010).
10. M. N. Uddin, J. Lau, *Adaptive-backstepping-based design of a nonlinear position controller for an IPMSM servo drive*, Electr. Comput. Eng. Can. J. Of, **32**, *2*, pp. 97–102 (2007).
11. F.-J. Lin, C.-C. Lee, "*Adaptive backstepping control for linear induction motor drive to track periodic references*, in Electric Power Applications, IEE Proceedings, 2000, **147**, pp. 449–458.
12. S. Heier, *Grid integration of wind energy conversion systems.* Wiley, 1998.
13. A. Rolan, A. Luna, G. Vazquez, D. Aguilar, G. Azevedo, *Modeling of a variable speed wind turbine with a Permanent Magnet Synchronous Generator*, in IEEE International Symposium on Industrial Electronics, 2009, pp. 734–739.
14 T. Ackermann, *Wind power in power systems*, **140**. Wiley Online Library, 2005.
15 R. Pena, J. C. Clare, G. M. Asher, *Doubly fed induction generator using back-to-back PWM converters and its application to variable-speed wind-energy generation*, IEE Proc.-Electr. Power Appl., **143**, *3*, pp. 231–241 (1996).
16. G. Abdelmadjid, B. S. Mohamed, T. Mohamed, S. Ahmed, M. Youcef, *An improved stator winding fault tolerance architecture for vector control of induction motor: Theory and experiment,* Electr. Power Syst. Res., **104**, pp. 129–137, (2013).
17. S. Heier, *Grid integration of wind energy: onshore and offshore conversion systems*. John Wiley & Sons, (2014).

18. A. Asri, Y. Mihoub, S. Hassaine, P. O. Logerais, A. Amiar, T. Allaou. *An adaptive fuzzy proportional integral method for maximum power point tracking control of permanent magnet synchronous generator wind energy conversion system*, in Rev. Roum. Sci. Techn.– Électrotechn. et Énerg. **63**, *3*, pp. 320–325, Bucharest, (2018).
19. A.Tahri, S. Hassaine, S. Moreau, *A robust control for permanent magnet synchronous generator associated with variable speed wind turbine*, **15**, *2*, pp. 1–8 (2015).
20. Z. Boudries, S. Tamalouz, *Study on sliding mode control of a small size wind turbine permanent magnet synchronous generator system*, in Rev. Roum. Sci. Techn.– Électrotechn. et Énerg. **64**, *2*, pp. 157–162, (2019).
21. A.Tahri, S.Hassaine, S.Moreau. *A hybrid active fault-tolerant control scheme for wind energy conversion system based on permanent magnet synchronous generator*. Archives of Electrical Engineering. **67**, *3*, pp.485-497, (2018).